Formation of clusters in the 2D *t–J* model: the mechanism for phase separation

2006 J. Phys.: Condens. Matter 18 4935

(http://iopscience.iop.org/0953-8984/18/20/017)

INSTITUTE OF PHYSICS PUBLISHING JOURNAL OF PHYSICS: CONDENSED MATTER

J. Phys.: Condens. Matter **18** (2006) 4935–4944 doi:10.1088/0953-8984/18/20/017

Formation of clusters in the 2D t–J model: the mechanism for phase separation

A Fledderjohann[1], A Langari[2,3] and K-H Mütter[1]

[1] Physics Department, University of Wuppertal, 42097 Wuppertal, Germany
[2] Department of Physics, Sharif University of Technology, Tehran 11365-9161, Iran

E-mail: langari@mpipks-dresden.mpg.de

Received 6 February 2006
Published 5 May 2006
Online at stacks.iop.org/JPhysCM/18/4935

Abstract

The emergence of phase separation is investigated in the framework of a 2D t–J model by means of a variational product ansatz, which covers the infinite lattice by two types of $L \times L$ clusters. Clusters of the first type are completely occupied with electrons, i.e. they carry maximal charge $Q_e = L^2$ and total spin 0, and thereby form the antiferromagnetic background. Holes occur in the second type of clusters—called 'hole clusters'. They carry a charge $Q_h < L^2$. The charge Q_h and the number $N(Q_h)$ of hole clusters is fixed by minimizing the total energy at given hole density and spin exchange coupling $\alpha = J/t$. For α not too small ($\alpha > 0.5$) it turns out that hole clusters are occupied with an even number $Q_h < L^2$ of electrons and carry a total spin 0. For increasing α the charge $Q_h(\alpha)$ of the hole clusters decreases. Some points on the boundary curve can be extracted from $Q_h(\alpha)$.

1. Introduction

Holes play a fundamental role in our understanding of high-T_c superconductivity [1]. The parent materials like La_2CuO_4 are insulators with antiferromagnetic order and doping with holes (missing electrons) opens the superconducting phase [2].

Experimental evidence has been found in $La_2CuO_{4+\delta}$ for phase separation [3–6]. This means that the holes in the CuO_2 planes are not distributed uniformly but concentrate in 'hole-rich' domains. The compound phase separates for $0.01 \leqslant \delta \leqslant 0.06$ below $T_{ps} \sim 300$ K into the nearly stoichiometric antiferromagnetic $La_2CuO_{4+\delta_1}$ with $\delta_1 < 0.02$ and Néel temperature ($T_N \simeq 250$ K), and a metallic superconducting oxygen-rich phase $La_2CuO_{4+\delta_2}$ with $\delta_2 \approx 0.02$ and $T_c \simeq 34$ K. The other evidence is related to the Sr-doped compound $La_{2-x}Sr_xCuO_{4+\gamma}$. This compound phase separates for $x \leqslant 0.03$ into the superconducting $La_{2-x}Sr_xCuO_{4+\gamma_1}$ ($\gamma_1 \approx 0.08$) and the nonsuperconducting $La_{2-x}Sr_xCuO_{4+\gamma_2}$ ($\gamma_2 \approx 0.00$) phases [7].

[3] Author to whom any correspondence should be addressed.

Intensive studies have been performed to understand this phenomenon in models for strongly correlated electrons like the Hubbard and t–J models. In the 2D t–J model, various attempts have been made to exploit the phase diagram in the plane spanned by the charge density $\rho = Q_{\rm tot}/N$ and the spin coupling $\alpha = J/t$ (N, $Q_{\rm tot}$ denote the total numbers of sites and electrons, respectively).

Phase separation occurs, if both the charge density ρ and the spin coupling α, are large enough:

$$1 \geqslant \rho \geqslant \rho_1, \qquad \alpha > \alpha_{\rm p}(\rho_1). \tag{1}$$

In this regime, the ground state can be represented by a product ansatz

$$\psi(\rho, N) = \psi_{\rm e}\big(N_{\rm e}(\rho)\big)\psi_h\big(N_h(\rho, \rho_1)\big) \tag{2}$$

of two clusters with site numbers $N_{\rm e}(\rho)$ and $N_h(\rho, \rho_1)$, which cover the whole lattice:

$$N_{\rm e}(\rho) + N_h(\rho, \rho_1) = N. \tag{3}$$

The $N_{\rm e}(\rho)$ sites in the 'electron' cluster are all occupied with electrons. The corresponding ground state $\psi_{\rm e}(N_{\rm e}(\rho))$ is just the ground state of the 2D Heisenberg model with $N_{\rm e}(\rho)$ sites. Holes occur in the 'hole' cluster with $N_h(\rho, \rho_1)$ sites. The corresponding ground state $\psi_h(N_h(\rho, \rho_1))$ is given by the t–J model with $N_h(\rho, \rho_1)$ sites and $Q_{\rm h} = N_h(\rho, \rho_1)\rho_1$ electrons. The numbers $N_{\rm e}(\rho)$ and $N_h(\rho, \rho_1)$ for the cluster sites are fixed by the total number of sites (3) and the total number of electrons

$$N_{\rm e}(\rho) + \rho_1 N_h(\rho, \rho_1) = Q_{\rm tot}. \tag{4}$$

From (2) to (4) one derives that the ground state energy per site

$$\varepsilon(\rho, \alpha) = \frac{1}{1 - \rho_1}\left[\varepsilon(\rho_1, \alpha)(1 - \rho) + \varepsilon(1, \alpha)(\rho - \rho_1)\right] \tag{5}$$

is linear in ρ. This holds for (1), i.e. in the region with phase separation.

The focus is the boundary curve $\alpha_{\rm p}(\rho_1)$ for phase separation. Two controversial points of view can be found in the literature. Emery *et al* [8] suggested that in the 2D t–J model the phase separation curve $\alpha_{\rm p}(\rho_1)$ starts at $\alpha_{\rm p}(\rho_1 = 1) = 0$, which means that phase separation exists already for low doping $(1 - \rho_1) \simeq 0$ and small values of α, as observed experimentally [3]. Their point of view is supported by Hellberg and Manousakis [9–12].

On the other hand, Putikka *et al* [13, 14] concluded, from a high-temperature expansion, that phase separation at low doping only emerges for larger α-values $\alpha > \alpha_{\rm p}(\rho_1 = 1) \simeq 1.2$, which would exclude the α regime realized in the experiments. This point of view is supported by DMRG calculations on ladders [15], variational wavefunctions of the Luttinger–Jastrow–Gutzwiller type [16], and Lanczos calculations [17, 18].

Finally, Green's function Monte Carlo simulations performed by Calandra *et al* (CBS) [19] led to a value $\alpha_{\rm p}(\rho_1 = 1) \simeq 0.5$.

In this paper, we would like to study the mechanism of phase separation by means of a product ansatz with $L \times L$ clusters of charge Q which cover the infinite lattice. Our method is in the spirit of the coupled cluster method (CCM) designed almost 50 years ago [20] as an approximation scheme for quantum many body problems. In order to handle the interaction between clusters, perturbative [21] and variational [22] methods have been implemented. In our study of the phase diagram in the $(\rho = Q/N, \alpha = J/t)$ plane, we proceed as follows: we start from the ground states $\psi^{(L)}(\rho_1, \alpha)$ with energies $E^{(L)}(Q_1, \alpha)$ on $L \times L$ clusters with charge $Q_1 = \rho_1 L^2$. These ground states can be computed analytically for plaquette clusters ($L = 2$). In section 2 we will discuss the product ansatz with plaquette clusters, which minimizes the total energy at fixed charge density $\rho = Q/N$. Phase separation can be observed on the small plaquette cluster on a 'microscopic scale'.

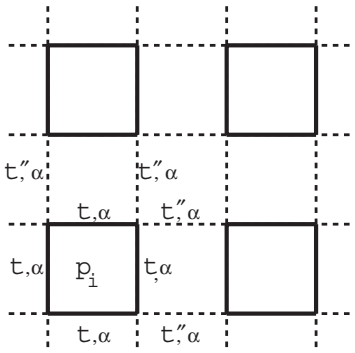

Figure 1. 2D lattice structure with underlying 2×2 plaquette structure.

In section 3 we extend our considerations to clusters of size $L \times L$. Results for the phase diagram obtained from a numerical calculation of ground state energies on a 4×4 cluster are shown. We finally summarize and present a discussion in section 4.

2. Plaquette cluster in the t–J model: phase separation *in statu nascendi*

We start from the t–J model in two dimensions which is built up as a lattice of $L \times L$ clusters (figure 1 for the example of $L = 2$):

$$H = t \sum_i h_{p_i}(\alpha = J/t) + t'' \sum_{\langle i,j \rangle} h_{p_i,p_j}(\alpha) \tag{6}$$

with h_{p_i} and h_{p_i,p_j} containing all nearest neighbour bonds $\langle k,l \rangle$ in a cluster p_i or between neighbouring clusters (p_i, p_j), respectively. In general, each nearest neighbour bond $\langle k,l \rangle$ of the lattice either belongs to a cluster (parameters t, $J = \alpha t$) or connects neighbouring clusters (t'', $J'' = \alpha t''$) and contributes with $t h^{(k,l)}(\alpha)$ or $t'' h^{(k,l)}(\alpha)$ to the respective intra- or inter-cluster part of the Hamiltonian (6):

$$h^{(k,l)}(\alpha) = \mathcal{P}\Big[-\sum_\sigma \left(c^+_{k,\sigma} c_{l,\sigma} + \text{h.c.}\right) + \alpha\Big(\mathbf{S}_k \cdot \mathbf{S}_l - \tfrac{1}{4} n_k n_l\Big)\Big]\mathcal{P} \tag{7}$$

where

$$n_l = \sum_\sigma n_{l,\sigma} = \sum_\sigma c^+_{l,\sigma} c_{l,\sigma} \tag{8}$$

and $\mathcal{P}$ projects onto the subspace where the occupation numbers n_l are restricted to zero or one. The electron spin operator is represented by $\mathbf{S}_k$ at the kth site.

The interaction between $L = 2$ clusters is mediated by the two dashed links for each spatial dimension. It is treated in the following by a perturbation expansion in the hopping parameter t'', which allows the hopping of electrons between neighbouring plaquettes.

To zeroth order in t'', the eigenstates of the 2D t–J model decay into a product

$$\prod_p |Q_p\rangle \tag{9}$$

of plaquette eigenstates $|Q_p\rangle$ with charge Q_p. The ground state is characterized by a minimum of the energy:

$$E_0 = \sum_p E^{(p)}(Q_p) = \sum_{Q=0}^{4} E^{(p)}(Q) N(Q) \tag{10}$$

where $N(Q)$ is the number of plaquettes with charge $Q = 0, 1, 2, 3, 4$. $E^{(p)}(Q)$ is the ground state energy of a plaquette with charge Q.

The numbers $N(Q)$ are constrained by the total number of plaquettes ($N/4$) and the total charge ($Q_{\rm tot}$):

$$\sum_{Q=0}^{4} N(Q) = N^{(p)} = \frac{N}{4}, \qquad \sum_{Q=0}^{4} QN(Q) = Q_{\rm tot}. \tag{11}$$

The plaquette ground state energies $E^{(\rm p)}(Q)$ have been computed in appendix A of [23]. The formulae obtained there simplify for the symmetric case we are considering here.

In the charge sectors $Q = 0, 1, 2, 4$ there is no level crossing and the plaquette ground state energy for all $\alpha > 0$ reads

$$E^{(\rm p)}(0) = 0 \qquad S = 0 \tag{12}$$

$$E^{(\rm p)}(1) = -2t \qquad S = 1/2 \tag{13}$$

$$E^{(\rm p)}(2) = -\frac{t}{2}\left(\alpha + \sqrt{\alpha^2 + 32}\right) \qquad S = 0 \tag{14}$$

$$E^{(\rm p)}(4) = -3t\alpha \qquad S = 0. \tag{15}$$

Note that the total spin $\mathbf{S}^{(\rm p)}$ of the plaquette electrons commutes with the plaquette Hamiltonian and the eigenvalues of ${\mathbf{S}^{(\rm p)}}^2 = S(S+1)$ can be used to characterize the plaquette ground state. This plays an important role in the sectors with $Q = 3$ where the ground state changes with α:

$$\begin{aligned} E^{(\rm p)}_{\rm I}(3,\alpha) &= -2t, \qquad S = 3/2 \qquad \text{for } 0 \leqslant \alpha \leqslant \alpha_{\rm m} \\ E^{(\rm p)}_{\rm II}(3,\alpha) &= -t\left(\alpha + \sqrt{\frac{\alpha^2}{4} + 3}\right), \qquad S = 1/2 \qquad \text{for } \alpha_{\rm m} \leqslant \alpha < 2 \\ E^{(\rm p)}_{\rm III}(3,\alpha) &= -t\left(\frac{3\alpha}{2} + 1\right), \qquad S = 1/2 \qquad \text{for } \alpha > 2 \end{aligned} \tag{16}$$

with $\alpha_{\rm m} = \frac{2}{3}(4 - \sqrt{13}) = 0.262\ldots$.

Note that the Nagaoka ferromagnetic state [24]—with maximal spin $S = Q/2$—is already visible on a four-site plaquette with one hole, i.e. $Q = 3$, if α is small enough: $\alpha < \alpha_{\rm m} = 0.262$. Eigenstates with maximal plaquette spin $S = Q/2$ exist in all charge channels; the corresponding energy eigenvalues $E(Q, S = Q/2)$ do not depend on the spin exchange coupling α. However, these eigenstates are not ground states except for the one-hole case.

Let us next look for the minimum of the total energy (10), which depends on the relative magnitude of the plaquette energies.

(a) In the regime where the inequality

$$E^{(\rm p)}(4) + E^{(\rm p)}(2) < 2E^{(\rm p)}(3) \tag{17}$$

holds, two plaquettes with charge $Q = 3$ are substituted by two plaquettes with charges $Q = 2$ and 4, respectively. Insertion of the ground state energies ((14), (15), (16)) yields the validity of (17) for

$$\alpha > \alpha(3) = \frac{2}{\sqrt{21}} \simeq 0.436. \tag{18}$$

(b) The inequality

$$E^{(\rm p)}(0) + E^{(\rm p)}(4) < 2E^{(\rm p)}(2) \tag{19}$$

holds for

$$\alpha \geqslant \alpha(2) = 4\sqrt{2/3} \simeq 3.266 \tag{20}$$

and allows the substitution of the charge $Q = 2$ plaquettes.

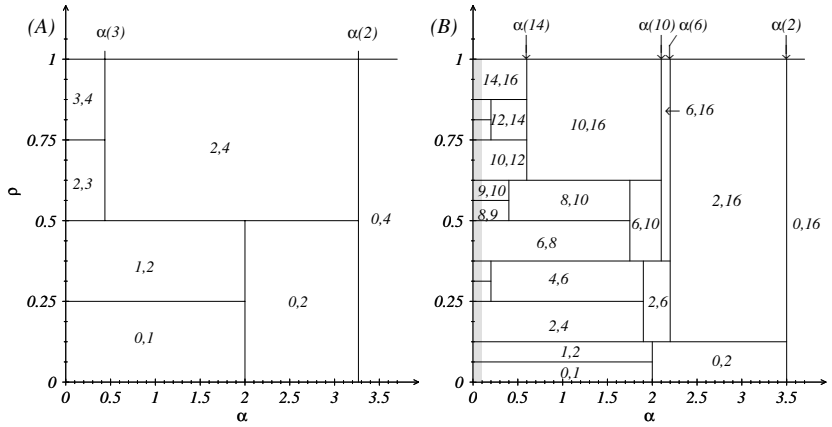

Figure 2. Schematic phase diagram obtained from 2×2 plaquettes (A) and 4×4 plaquettes (B). The charges Q_1, Q_2 that constitute the respective ground states in the ρ–α-planes and the boundaries $\alpha(2j)$ are given in the text.

(c) The inequality

$$E^{(\mathrm{p})}(0) + E^{(\mathrm{p})}(2) < 2E^{(\mathrm{p})}(1) \tag{21}$$

holds for

$$\alpha > 2 \tag{22}$$

and allows one to substitute $Q = 1$ plaquettes.

Figure 2(A) shows a schematic view of the phase diagram in the ρ–α plane with the pairs of plaquette charges, which fix the ground state energy per site according to equations (10) and (11).

In each of the domains with plaquette pairs Q_1, Q_2

$$Q_1 < Q_2 \qquad \frac{Q_1}{N_c} < \rho < \frac{Q_2}{N_c} \tag{23}$$

with $N_c = 4$, the ground state energy per site

$$\varepsilon(\rho,\alpha) = \frac{1}{Q_2 - Q_1}\left\{E^{(\mathrm{p})}(Q_1)\left(\frac{Q_2}{N_c} - \rho\right) + E^{(\mathrm{p})}(Q_2)\left(\rho - \frac{Q_1}{N_c}\right)\right\} \tag{24}$$

is linear in ρ and the chemical potential $\mu(\rho,\alpha) = \mathrm{d}\varepsilon/\mathrm{d}\rho$ is constant with respect to ρ. Note that two domains (Q_1, Q_2) and (Q_2, Q_3) with a common plaquette charge Q_2 have also a common horizontal boundary at charge density $\rho_2 = Q_2/4$. At this boundary the chemical potential $\mu(\rho,\alpha)$ as a function of ρ is discontinuous with a jump

$$\begin{aligned}\Delta(Q_2,\alpha) &= \mu(\rho+0,\alpha) - \mu(\rho-0,\alpha)\\ &= \frac{E^{(\mathrm{p})}(Q_3)}{Q_3 - Q_2} + \frac{E^{(\mathrm{p})}(Q_1)}{Q_2 - Q_1} - \frac{Q_3 - Q_1}{(Q_3 - Q_2)(Q_2 - Q_1)}E^{(\mathrm{p})}(Q_2)\end{aligned} \tag{25}$$

which vanishes for a specific value of $\alpha = \alpha(Q_2)$. These values define the vertical lines in the phase diagram given by (18), (20) and (22). This type of phase diagram was introduced first by Kagan *et al* [25] for the three-leg ladder in the rung cluster approximation. Note that the constraints for $(N^{(\mathrm{p})}, Q_{\mathrm{tot}})$ (11) are taken into account explicitly on both sides of the inequalities (17), (19), (21). This procedure can be considered as an alternative to the usual grand canonical one, where the charge conservation constraint (11) is eliminated by a reservoir with a fixed chemical potential.

3. Product ansatz for the ground state with large clusters

The considerations which led to the phase diagram in figure 2(A) based on plaquette clusters can easily be extended to larger $L \times L = N_c$ clusters with N_c sites and charges $Q = N_c, \ldots, 0$. We start with the ground state energies $E(Q, N_c, \alpha)$ and their dependence on α. The generalization of (24) to a cluster with N_c sites and charges $Q_1 < Q_2$ is straightforward by replacing $E^{(\mathrm{p})}(Q_1) \to E(Q_1, \alpha, N_c)$. Again the ground state energy per site is linear in ρ and the chemical potential is constant:

$$\mu(\rho, \alpha) = \frac{1}{Q_2 - Q_1}\Big\{E(Q_2, \alpha, N_c) - E(Q_1, \alpha, N_c)\Big\}. \tag{26}$$

Two domains (Q_1, Q_2) (Q_2, Q_3) with a common cluster charge Q_2 have a common boundary in the phase diagram at $\rho_2 = Q_2/N_c$. At this boundary the chemical potential is discontinuous with a jump

$$\Delta(Q_2, \alpha) = \mu(\rho_2 + 0, \alpha) - \mu(\rho_2 - 0, \alpha) = \frac{E(Q_3) - E(Q_2)}{Q_3 - Q_2} - \frac{E(Q_2) - E(Q_1)}{Q_2 - Q_1} \tag{27}$$

which vanishes for a specific value of $\alpha = \alpha(Q_2)$. The inequality

$$\Delta(Q_2, \alpha) < 0 \qquad \text{for } \alpha > \alpha(Q_2) \tag{28}$$

means that the clusters with charge Q_2 and ground state energy $E(Q_2, \alpha, N_c)$ can be substituted by clusters with charges Q_3 and Q_1 and energies $E(Q_3, \alpha, N_c)$, $E(Q_1, \alpha, N_c)$. Here the two domains (Q_1, Q_2) (Q_2, Q_3) merge for $\alpha > \alpha(Q_2)$ and the ground state is given by a cluster product ansatz with charges (Q_1, Q_3).

Let us first consider the case (case (A))

$$Q_1 = Q_2 - 1, \qquad Q_3 = Q_2 + 1, \qquad Q_2 \text{ odd}, \qquad \alpha < \alpha(Q_2). \tag{29}$$

Here the ground state is built up from clusters with charges:

$$(Q_2 - 1, Q_2) \qquad \text{for } \frac{Q_2 - 1}{N_c} \leqslant \rho \leqslant \frac{Q_2}{N_c} \tag{30}$$

$$(Q_2, Q_2 + 1) \qquad \text{for } \frac{Q_2}{N_c} \leqslant \rho \leqslant \frac{Q_2 + 1}{N_c}. \tag{31}$$

The vanishing of the jump (27) in the chemical potential

$$\Delta(Q_2, \alpha(Q_2)) = E(Q_2 + 1) + E(Q_2 - 1) - 2E(Q_2) = 0 \tag{32}$$

defines the boundary $\alpha = \alpha(Q_2)$, where the two domains (30) and (31) merge together:

$$(Q_2 - 1, Q_2 + 1) \qquad \text{for } \frac{Q_2 - 1}{N_c} \leqslant \rho \leqslant \frac{Q_2 + 1}{N_c} \qquad \text{and} \qquad \alpha > \alpha(Q_2). \tag{33}$$

The numerical evaluation of (32) from the ground state energies on a $4 \times 4 = 16$ cluster—with periodic boundary conditions—yields the couplings $\alpha(Q_2)$ listed in table 1 (columns 1, 2).

In the next step, we consider the following cluster charges (case (B)):

$$Q_1 = Q_2 - 2, \qquad Q_3 = Q_2 + 2, \qquad Q_2 = 14, 12, 8, 4, \qquad \alpha < \alpha(Q_2). \tag{34}$$

Here the ground state is built up from clusters with charges

$$(Q_2 - 2, Q_2) \qquad \text{for } \frac{Q_2 - 2}{N_c} \leqslant \rho \leqslant \frac{Q_2}{N_c} \tag{35}$$

$$(Q_2, Q_2 + 2) \qquad \text{for } \frac{Q_2}{N_c} \leqslant \rho \leqslant \frac{Q_2 + 2}{N_c}. \tag{36}$$

Table 1. Boundary couplings $\alpha(Q_2)$ (from left to right cases (A), (B), (C)) where the jump (27) in the chemical potential vanishes for cases (Q_1, Q_2, Q_3).

(Q_1, Q_2, Q_3)	$\alpha(Q_2)$	(Q_1, Q_2, Q_3)	$\alpha(Q_2)$	(Q_1, Q_2, Q_3)	$\alpha(Q_2)$
(14, 15, 16)	<0.1	(12, 14, 16)	0.6	(6, 10, 16)	2.1 . . .
(12, 13, 14)	0.2	(10, 12, 14)	0.6	(2, 6, 16)	2.2 . . .
(10, 11, 12)	<0.1	(6, 8, 10)	1.74	(0, 2, 16)	3.5 . . .
(8, 9, 10)	0.4	(2, 4, 6)	1.9		
(6, 7, 8)	<0.1				
(4, 5, 6)	0.2				
(2, 3, 4)	<0.1				
(0, 1, 2)	2.0				

The vanishing of the jump (27) in the chemical potential

$$\Delta(Q_2, \alpha(Q_2)) = \tfrac{1}{2}\,[E(Q_2+2) + E(Q_2-2) - 2E(Q_2)] = 0 \tag{37}$$

again defines the boundary $\alpha = \alpha(Q_2)$, where the two domains (35) and (36) merge together:

$$(Q_2-2,\, Q_2+2) \qquad \text{for } \frac{Q_2-2}{N_c} \leqslant \rho \leqslant \frac{Q_2+2}{N_c} \qquad \text{and} \qquad \alpha > \alpha(Q_2). \tag{38}$$

The numerical evaluation of (37) from the ground state energies on a $4 \times 4 = 16$ cluster—with periodic boundary conditions—yields the couplings $\alpha(Q_2)$ listed in table 1 (columns 3, 4).

We are left with clusters of charge $Q_2 = 10, 6, 2$ (case (C)).

They are eliminated successively by considering the jumps (27) in the chemical potential for the cases in table 1 (columns 5, 6). These jumps vanish at the couplings $\alpha = \alpha(Q_2)$ listed in the third column, such that the clusters with charges Q_2 can be eliminated for $\alpha > \alpha(Q_2)$. The resulting phase diagram is shown in figure 2(B). The pairs of integers in the rectangular domains denote the two cluster charges which determine the ground state in the product ansatz.

Let us comment on the appropriate boundary conditions for the $L \times L$ cluster in the variational product ansatz for the ground state on the infinite lattice. *A priori* we are free in our choice of the clusters and their boundary conditions. In our opinion periodic boundary conditions are most appropriate for the following reasons.

The variational product ansatz becomes exact in the limit of infinite cluster ($L \to \infty$, $N_c = L^2 \to \infty$). In this case, the cluster energies $E(Q, \alpha, N_c) = N_c \varepsilon(\rho_1 = Q/N_c, \alpha)$ are related to the ground state energies per site $\varepsilon(\rho_1 = Q/N_c, \alpha)$ at fixed charge density. On finite clusters with $L \times L = N_c$ sites the ground state energies are approximated most accurately with periodic boundary conditions, since the interaction between the clusters is partly taken into account by means of the periodic boundary terms. Of course—in a perturbation expansion for the interaction between the clusters—the periodic boundary terms have to be subtracted again in each order of a standard perturbation treatment.

4. Summary and discussion

In this paper we have made an attempt to describe phase separation in terms of a product cluster ansatz for the ground state of the 2D t–J model.

The analytic results for 2×2 plaquette clusters reveal already the gross features as depicted in the phase diagram in figure 2. For ρ and α large enough the ground state is built up from two types of plaquettes $(Q_\mathrm{h}, Q_\mathrm{e}) = (0, 4), (2, 4)$. The hole clusters carry a charge Q_h which

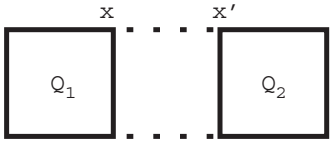

Figure 3. Interaction between neighbouring plaquettes with charges Q_1, Q_2 shown for a pair of nearest neighbour sites x and x'.

Table 2. Points on the boundary curve (1) for phase separation derived from a 4×4 cluster.

$\rho_1 = Q_h/16$	0	1/8	3/8	5/8
$\alpha_p(\rho_1)$	3.5	2.2	2.1	0.6

increases with decreasing α:

$$Q_h = 0 \qquad \alpha(2) = 4\sqrt{\frac{2}{3}} < \alpha \qquad 0 \leqslant \rho \leqslant 1 \tag{39}$$

$$Q_h = 2 \qquad \alpha(3) = \frac{2}{\sqrt{21}} \leqslant \alpha \leqslant \alpha(2) \qquad \frac{1}{2} \leqslant \rho \leqslant 1 \tag{40}$$

where $\rho_1 = Q_h/N$ denotes the charge density in the hole cluster. The second type of plaquette is completely occupied with electrons $Q_e = 4$.

In the regimes (39) and (40) the ground state energy per site (24) is linear in ρ in the respective intervals. The lower bounds in the α-intervals listed in (39), (40) define two points on the boundary (1) for phase separation:

$$\alpha_p(\rho_1 = 0) = 4\sqrt{\frac{2}{3}}, \qquad \alpha_p\left(\rho_1 = \frac{1}{2}\right) = \frac{2}{\sqrt{21}}. \tag{41}$$

The numerical results—obtained from a product ansatz with 4×4 clusters—lead to the phase diagram in figure 2(B) similar to 2(A) for 2×2 clusters. In each rectangular domain the cluster charges Q_1, Q_2 result from a minimization of the ground state energy per site (24) at fixed charge density ρ (in the infinite system). Phase separation is observed in the upper part of figure 2(B) with cluster charges $(Q_h, Q_e) = (0, 16), (2, 16), (6, 16), (10, 16)$ The charge Q_h of the hole clusters changes with the spin exchange coupling α:

$$Q_h = 0 \qquad \alpha(2) = 3.5 < \alpha, \qquad 0 \leqslant \rho \leqslant 1 \tag{42}$$

$$Q_h = 2 \qquad \alpha(6) = 2.2 < \alpha < \alpha(2), \qquad \tfrac{1}{8} \leqslant \rho \leqslant 1 \tag{43}$$

$$Q_h = 6 \qquad \alpha(10) = 2.1 < \alpha < \alpha(6), \qquad \tfrac{3}{8} \leqslant \rho \leqslant 1 \tag{44}$$

$$Q_h = 10 \qquad \alpha(14) = 0.6 < \alpha < \alpha(10), \qquad \tfrac{5}{8} \leqslant \rho \leqslant 1. \tag{45}$$

The ground state energy per site (24) is linear in the ρ intervals listed in (42)–(45). The lower bounds in the α intervals yield four points on the boundary curve (1) for phase separation shown in table 2:

The product ansatz ((9) for plaquettes) with isolated cluster ground states is highly degenerate. Each distribution of electron and hole clusters over the whole lattice leads to the same ground state energy, if we neglect the interaction between neighbouring clusters (figure 3).

Let us denote the interaction energy between neighbouring clusters with charges $Q_2 = L^2$, $Q_1 = Q_h$ by $W(Q_1, Q_2)$ (figure 3). If the difference

$$\Delta = W(L^2, L^2) + W(Q_h, Q_h) - 2W(Q_h, L^2) < 0 \tag{46}$$

is negative, the ground state prefers phase separation in the following sense. The numbers $N(L^2, L^2)$, $N(Q_h, Q_h)$ of identical neighbouring clusters is maximal:

$$\frac{N(L^2, L^2)}{N} = 2\frac{N(L^2)}{N}, \qquad \frac{N(Q_h, Q_h)}{N} = 2\frac{N(Q_h)}{N} \qquad \text{for } N \to \infty \tag{47}$$

where $N(L^2)$ and $N(Q_h)$ are the numbers of electron and hole clusters, respectively. As a consequence the number of neighbouring clusters $N(Q_h, L^2)$ with different charges is minimal:

$$\frac{N(Q_h, L^2)}{N} \to 0 \qquad \text{for } N \to \infty. \tag{48}$$

Within the product ansatz (9) with plaquettes of charge $Q_2 = L^2$, $Q_1 = Q_h$ the interaction energies turn out to be

$$W(Q_1, Q_2) = \sum_x \langle Q_1, Q_2 | h^{(x,x')} | Q_1, Q_2 \rangle = -\frac{\alpha}{32} Q_1 Q_2, \qquad (L = 2), \tag{49}$$

provided that the cluster charges are even and the total cluster spins are zero. In this case the spin matrix elements

$$\langle Q_1 | \mathbf{S}_x | Q_1 \rangle = \langle Q_2 | \mathbf{S}_x | Q_2 \rangle = 0 \tag{50}$$

and the hopping contributions arising in (7) vanish for $L^2 - Q_h \geqslant 2$. Equation (49) implies that the inequality (46) is valid and the ground state configuration (47), (48) with two big clusters of charge density $\rho_2 = 1$, $\rho_1 = Q_h/L^2$ is selected out. According to (42)–(45) the necessary condition $L^2 - Q_h \geqslant 2$ is satisfied for $\alpha > 0.6$.

The phase diagrams in figures 2(A) and (B) contain the whole information on the ground state of the system provided that a product ansatz with two $L \times L$ clusters and charges Q_1, Q_2 is adequate. Since we know the cluster ground states in each charge sector from the analytical calculation in [23] for $L = 2$ and our numerical calculation for $L = 4$, we can also determine the hole–hole correlators:

$$C_{(x,y)}(Q_1) = \langle n_h(0,0) n_h(x,y) \rangle - \langle n_h(0,0) \rangle \langle n_h(x,y) \rangle \tag{51}$$

where $n_h(0,0)$, $n_h(x,y)$ count the number of holes at sites $(0,0)$ and (x,y).

On the 4×4 cluster with periodic boundary conditions five independent correlators can be arranged according to the distance vector (x,y). Let us look at the following regime:

$$2.2 \leqslant \alpha \leqslant 3.5, \qquad \tfrac{1}{8} \leqslant \rho \leqslant 1. \tag{52}$$

According to the phase diagram in figure 2(B) the ground state contains clusters with charges $Q_1 = 2$, $Q_2 = 16$. The hole–hole correlators (51) in the $Q_1 = 2$ cluster turn out to be negative. However, the modulus of $|C_{1,0}(\alpha)|$ decreases with α, whereas $|C_{2,0}(\alpha)|$, $|C_{2,1}(\alpha)|$ and $|C_{2,2}(\alpha)|$ increase with α. We interpret these increasing 'long'-range correlations as a hint to condensation of holes for large α-values.

Next let us look for the hole–hole correlators in the α-regime

$$0.6 \leqslant \alpha \leqslant 2.1, \qquad \tfrac{5}{8} \leqslant \rho \leqslant 1. \tag{53}$$

According to the phase diagram in figure 2(B) the ground state contains clusters with charges $Q_1 = 10$, $Q_2 = 16$. Again all correlators are negative. The 'long'-range correlators $|C_{2,0}| = |C_{1,1}|$, $|C_{2,1}|$, $|C_{2,2}|$ are small in comparison with the nearest neighbour correlator $|C_{1,0}|$ for $0.6 \leqslant \alpha \leqslant 1.5$. In this regime the system prefers formation of hole pairs on neighbouring sites.

On the other hand for $\alpha < 0.6$ and $\rho > 0.75$, we observe rapid changes of the ground state with ρ and α as is indicated by the numerous small rectangular domains in the left upper part in

figure 2(B). In this regime holes are no longer confined, as can be seen directly from the product ansatz with 2×2 plaquettes and charges $Q_h = 3$, $Q_e = 4$ (upper left part in figure 2(A)). Here, the hopping matrix elements (7) are active already in first-order perturbation theory and allow for the exchange of hole ($Q_h = 3$) and electron ($Q_e = 4$) clusters. In principle, the holes can now hop over the whole lattice and destroy thereby phase separation. The distribution of the holes can be determined only from a precise computation of the ground state in the low-doping δ, low-α regime.

References

[1] Bednorz J G and Müller K A 1986 *Z. Phys.* B **64** 189
[2] Anderson P W 1987 *Science* **235** 1196
[3] Jorgensen J D, Dabrowski B, Pei S, Hinks D G and Soderholm L 1988 *Phys. Rev.* B **38** 11337
[4] Hammel P C *et al* 1990 *Phys. Rev.* B **42** 6781
[5] Hammel P C *et al* 1991 *Physica* C **185–189** 1095
[6] Chou F C *et al* 1996 *Phys. Rev.* B **54** 572
[7] Cho J H *et al* 1993 *Phys. Rev. Lett.* **70** 222
[8] Emery V J, Kivelson S A and Lin H Q 1990 *Phys. Rev. Lett.* **64** 475
[9] Hellberg C S and Manousakis E 1995 *Phys. Rev.* B **52** 4639
[10] Hellberg C S and Manousakis E 1997 *Phys. Rev. Lett.* **78** 4609
[11] Hellberg C S and Manousakis E 1999 *Phys. Rev. Lett.* **83** 132
[12] Hellberg C S and Manousakis E 2000 *Phys. Rev.* B **61** 11787
[13] Putikka W O, Luchini M U and Rice T M 1992 *Phys. Rev. Lett.* **68** 538
[14] Putikka W O, Glenister R L, Singh R R P and Tsunetsugu H 1994 *Phys. Rev. Lett.* **73** 170
[15] Rommer S, White S R and Scalapino D J 2000 *Phys. Rev.* B **61** 13424
[16] Valenti R and Gros C 1992 *Phys. Rev. Lett.* **68** 2402
[17] Dagotto E, Moreo A, Ortolani F, Poilblanc D and Riera J 1992 *Phys. Rev.* B **45** 10741
[18] Dagotto E, Martins G B, Riera J, Malvezzi A L and Gazza C 1998 *Phys. Rev.* B **58** 12063
[19] Calandra M, Becca F and Sorella S 1998 *Phys. Rev. Lett.* **81** 5185
[20] Coester F 1958 *Nucl. Phys.* **7** 421
Coester F and Kümmel K H 1960 *Nucl. Phys.* **17** 477
[21] Gros C and Valenti R 1993 *Phys. Rev.* B **48** 418
Sénéchal D, Perez D and Pioro-Ladrière M 2000 *Phys. Rev. Lett.* **84** 522
Sénéchal D, Perez D and Plouffe D 2002 *Phys. Rev.* B **66** 075129
[22] Potthoff M 2003 *Eur. Phys. J.* B **32** 429
Potthoff M 2003 *Phys. Rev. Lett.* **91** 206402
[23] Fledderjohann A, Langari A and Mütter K H 2004 *J. Phys.: Condens. Matter* **16** 8571
[24] Nagaoka Y 1966 *Phys. Rev.* **147** 392
[25] Kagan M Y, Haas S and Rice T M 1999 *Physica* C **317** 185